Astron. Astrophys. 240, 116–122 (1990)

ASTRONOMY AND ASTROPHYSICS

The 44 GHz methanol masers: results of an extensive survey in the $7_0 \rightarrow 6_1 A^+$ line

R. Bachiller[1], K.M. Menten[2], J. Gómez-González[1], and A. Barcia[1]

[1] Centro Astronómico de Yebes, O.A.N., Apartado 148, E-19080 Guadalajara, Spain
[2] Harvard–Smithsonian Center for Astrophysics, 60 Garden Street, Cambridge, MA 02138, USA

Received February 5, accepted April 30, 1990

Abstract. We conducted a search for emission in the 44 GHz $7_0 \rightarrow 6_1 A^+$ transition of CH_3OH toward 124 known water masers associated with star forming regions and evolved stars. Emission was detected toward 16 sources. In most sources maser action is observed, indicated by narrow, intense spectral features. The methanol maser velocities are similar to the systemic velocities of the regions in question and show no high-velocity features. Several new maser components where found in regions containing previously known methanol masers.

Key words: methanol – masers – molecular clouds – star formation

1. Introduction

Recently, a number of cm- and mm-wavelength transitions of the methanol (CH_3OH) molecule have been found to show strong maser action toward molecular cloud regions containing sites of active star formation. Clearly, all methanol masers found so far belong to one of two classes (Menten 1987; Batrla et al. 1987): Class A methanol masers are generally found offset by up to ≈ 1 pc from compact H II regions, infrared sources, OH masers and H_2O maser centers, while interferometric studies have shown that Class B sources are coexistent with OH masers and appear projected against ultracompact H II regions (Menten et al. 1988a, b). The most prominent transition observed toward Class B sources is the widespread 12 GHz $2_0 \rightarrow 3_{-1} E$ line (Batrla et al. 1987); several other Class B transitions have been observed (Wilson et al. 1984, 1985; Haschick et al. 1989). Class A masers are not masing in any of the last mentioned lines, rather they show absorption in the 12 GHz line and maser emission in the series of $J_{k=2} \rightarrow J_{k=1} E$ transitions near 25 GHz (Menten et al. 1986), the 36 GHz $4_{-1} \rightarrow 3_0 E$ line (Morimoto et al. 1985; Haschick & Baan 1989), and the $5_{-1} \rightarrow 4_0 E$ and $8_0 \rightarrow 7_1 A^+$ transitions at 84 and 95 GHz, respectively (Batrla & Menten 1988; Plambeck & Wright 1988). The Class A methanol maser transition that seems to be most widespread and generally shows the strongest emission is the $7_0 \rightarrow 6_1 A^+$ line near 44 GHz. Masers in this transition were first detected by Morimoto et al. (1985) toward the Sgr B2 and W 51 regions. During a recent survey, about 20 additional $7_0 \rightarrow 6_1 A^+$ masers were found (Haschick et al. 1990), many of them toward positions where masers in one or more of the other Class A transitions mentioned above had been observed previously.

In order to obtain more information on the frequency of occurrence of Class A methanol masers, we used the 14-m telescope of Yebes Observatory to search for maser emission in the $7_0 \rightarrow 6_1 A^+$ transition.

2. Observations

The observations were made under generally good weather conditions in December 1988 and January 1989 with the 14-m telescope of the Centro Astronómico de Yebes near Guadalajara, Spain. The receiver was a cooled Schottky mixer with a double-sideband (DSB) receiver temperature of about 70 K. The DSB system temperatures ranged between 170 and 230 K, depending on the weather and the elevation of the observed sources. At the observing frequency of 44 069.43 MHz the aperture efficiency of the antenna is 0.17 and the beam size 2′, so that 1 K antenna temperature corresponds to a flux density of 90 Jy. The pointing was checked by observations of planets and found to be accurate to 20″. Errors in the absolute calibration are estimated to be smaller than 20%. The spectrometer was a 256×50 kHz filter bank that gave a spectral resolution of 0.34 km s^{-1}. The observations were made in frequency switching mode. Typical observing times were of order 10–20 minutes per source, resulting in rms noise levels of 3–5 Jy per frequency channel.

3. Results

Our source list consisted of galactic H II regions, late-type stars, and dark cloud regions containing H_2O masers. Positions are taken from the recently published water maser catalogue of Cesaroni et al. (1988). We also use these authors' nomenclature and refer to their catalogue for information on the nature of the observed sources and references to the relevant H_2O literature. Furthermore, we searched for the $7_0 \rightarrow 6_1 A^+$ line toward a number of ultra-compact H II regions from the sample of Wood & Churchwell (1989).

In total 124 sources were observed. The line was detected toward 16 sources all of which lie in the vicinity of H II regions. Line parameters determined from Gaussian fits are given in Table 1. Observed spectra are shown in Figs. 1 and 2. For a number of sources, limited maps were made, typically five points

Send offprint requests to: K.M. Menten

Table 1. Line parameters determined from $7_0 \rightarrow 6_1 A^+$ observations

Source	α_{1950}	δ_{1950}	$\int S dv$ (Jy km s^{-1})	v_{LSR} (km s^{-1})	Δv (km s^{-1})	Notes
W 3 (3)	$02^h22^m06^s.1$	61°50′40″	10 (2)	−38.40 (0.07)	0.7 (0.1)	
S 231	05 35 51.3	35 44 16	14 (2)	−16.67 (0.04)	0.55 (0.07)	
G 5.89−0.39	17 57 26.8	−24 03 54	53 (5)	8.77 (0.06)	1.4 (0.2)	a, b
			40 (5)	12.17 (0.07)	1.2 (0.2)	
G 10.30−0.15	18 05 57.9	−20 06 26	29 (7)	13.8 (0.2)	2.3 (0.7)	c
G 11.94−0.62	18 11 04.4	−18 54 20	17 (4)	35.19 (0.05)	0.5 (0.1)	a, c
			75 (3)	35.8 (0.3)	4.1 (0.6)	
M 17 (3)	18 17 31.0	−16 12 50	25 (6)	18.9 (0.2)	2.3 (0.9)	
G 19.61−0.23	18 24 50.3	−11 58 34	23 (4)	41.43 (0.07)	0.8 (0.2)	
W 42	18 33 30.3	−07 14 42	47 (6)	114.5 (0.1)	1.8 (0.3)	
G 29.96−0.02	18 43 27.1	−02 42 36	18 (4)	98.5 (0.1)	1.3 (0.3)	d
G 35.05−0.52	18 54 37.1	01 35 01	26 (2)	49.94 (0.03)	1.0 (0.1)	
G 35.20−0.74	18 55 40.8	01 36 30	81 (5)	34.2 (0.1)	3.9 (0.4)	
ON 2	20 19 50.0	37 16 30	42 (3)	−2.00 (0.08)	2.3 (0.2)	e
DR 21	20 37 12.6	42 08 46	32 (3)	−3.67 (0.03)	0.64 (0.07)	f
W 75 S (3)	20 37 16.7	42 15 15	22 (3)	−5.22 (0.03)	0.7 (0.1)	g
			31 (3)	−3.46 (0.08)	1.6 (0.2)	
			18 (3)	0.25 (0.08)	1.2 (0.2)	
R 146	21 42 40.0	65 52 57	16 (4)	−6.4 (0.1)	1.1 (0.3)	
NGC 7538	23 11 36.7	61 11 49	52 (3)	−57.35 (0.03)	1.13 (0.07)	

Notes: Errors are 1σ deviations determined by Gaussian fits. The spectra were obtained with a velocity resolution of 0.34 km s^{-1}. Positions given are formal (0, 0) positions of our observations and not necessarily the actual maser positions. In several cases offset positions were measured to allow a more accurate determination of the maser position (see discussion in text)
(a) Two independent Gaussians fitted
(b) Source also known as W 28 A2(1)
(c) Source position taken from Wood and Churchwell (1989)
(d) Source also known as W 43 S
(e) Observed position is offset by (13″, 38″) and (−21″, −31″) from the ON 2 S and ON 2 N water maser centers, respectively
(f) Position given is located 60″ east of the strong maser feature (DR 21−West) detected by Haschick et al. (1990) at a velocity of −2.47 km s^{-1}
(g) Three independent Gaussians fitted

around the nominal position at half-beam spacing, in order to determine the source position. Since for most sources significantly more integration time was spent on the center position, the spectra taken toward the offset positions usually have a much lower signal-to-noise ratio than the spectra of the center position. Because of this, in several cases the line was not detected toward the offset positions, making an accurate position determination impossible. Of course it is clear that in these cases the emission arises from close to the center position.

For the sources toward which no emission was detected, upper limits on the flux density are given in Table 2. Additionally, a number of regions were observed toward which Haschick et al. (1990) report maser emission in the $7_0 \rightarrow 6_1 A^+$ line. Within the errors, our results are consistent with theirs and therefore not listed in the present paper (but see the discussion for DR 21 and NGC 7538). We just mention that no significant intensity variations have taken place within the several month period between the observations conducted by Haschick et al. and our measurements. This fact is consistent with the result that to date no time variability has been observed in *any* methanol maser line (Menten et al. 1988c and personal communication).

Note also that a number of weak sources toward which Haschick et al. report emission were not detected by us because of the lower sensitivity of our observations. In these cases our upper limits (listed in Table 2) are consistent with the intensities observed by Haschick et al.

We did not detect the $7_0 \rightarrow 6_1 A^+$ line toward any one of the late-type stars observed by us. In fact, no detection of methanol has ever been reported toward a late-type star, despite several searches (Menten et al. 1986; Norris et al. 1987).

4. Discussion

4.1. Notes on selected sources

4.1.1. G 5.89−0.39 (= W 28 A2)

We detect two intense narrow maser components toward the compact H II region G 5.89−0.39 (Wood & Churchwell 1989).

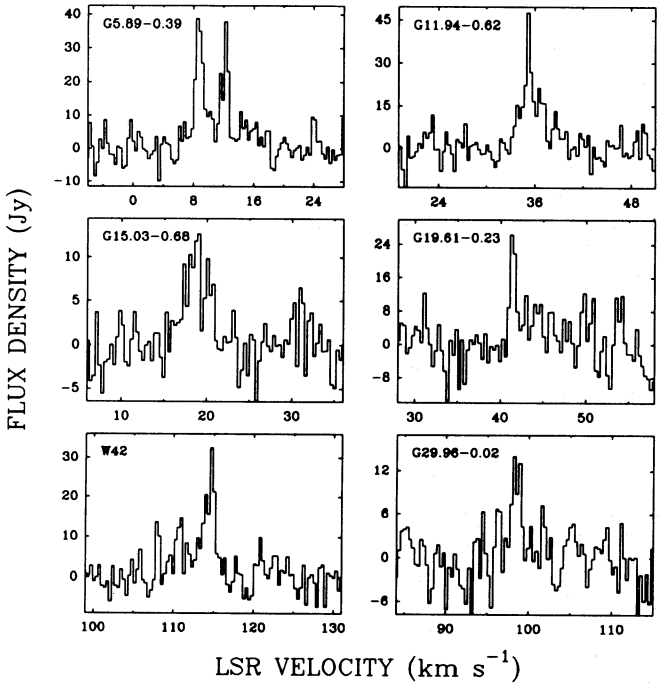

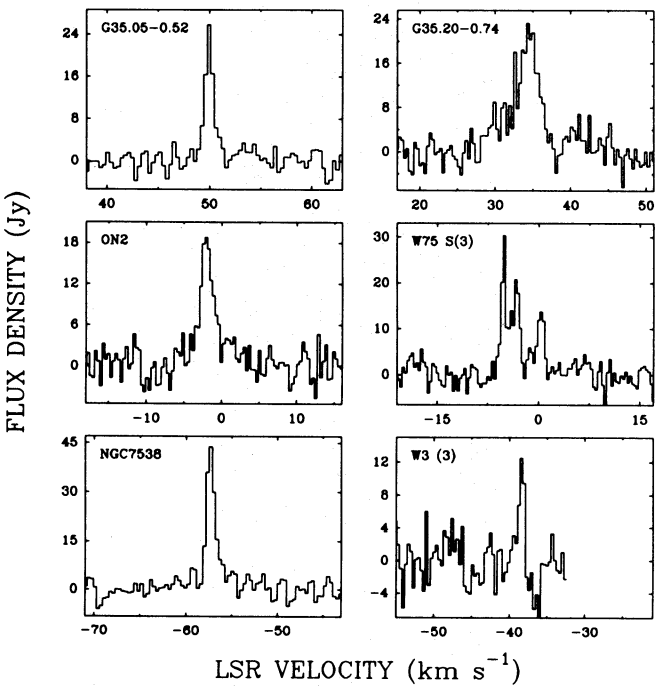

Fig. 1. (continued)

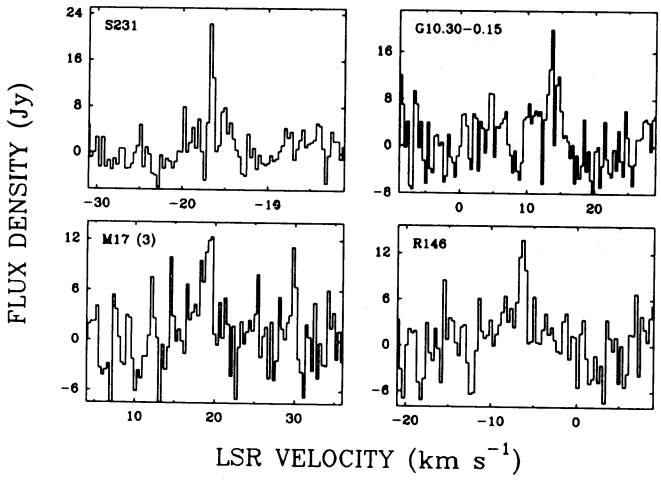

Fig. 1. Spectra of the $7_0 \rightarrow 6_1 A^+$ transition of CH_3OH observed toward various galactic star forming regions. The observed positions are given in Table 1. The velocity resolution is 0.34 km s^{-1} in all cases

This source is at the center of a powerful molecular outflow observed in high velocity CO emission (Harvey & Forveille 1988) and molecular hydrogen emission (Oliva & Moorwood 1986). Water waters are centered at two locations, one of which (W 28 A(1)) is coincident with our nominal observing position (Table 1), while the other one, A(2), is found 18″ to the south (Genzel & Downes 1977). The velocities of the methanol maser features are close to the centroid velocity of the H_2O maser emission, which is at 14 km s^{-1}, but the methanol spectrum shows neither the complexity nor the wide velocity spread of the H_2O emission. Our offset measurements indicate that both velocity components observed in the methanol line are located close to the H II region.

4.1.2. G 10.30–0.15 and G 11.94–0.62

To date, neither OH nor H_2O maser emission has been reported toward these ultracompact HII regions (Wood & Churchwell 1989). Toward G 11.94–0.62 clearly a narrow feature is observed together with broader emission.

4.1.3. M 17

In the M 17 star forming region we observed the position of the water maser M 17(3), which was found by Genzel and Downes (1977) near the ultracompact H II region detected by Felli et al. (1980). The $7_0 \rightarrow 6_1 A^+$ line is marginally detected with a linewidth that is similar to the widths of ammonia lines observed in this region (Güsten & Fiebig 1988), which indicates that we are possibly observing thermal mission. The NH_3 and CH_3OH radial velocities also are similar. Assuming a methanol rotation temperature of 50 K, a value comparable to the kinetic temperature Güsten and Fiebig derive from their NH_3 observations, assuming that the source fills the telescope beam, and using the formula given by Haschick et al. (1990), we calculate a CH_3OH column density of $8\,10^{15}$ cm^{-2}. Because of the measurement uncertainties and the unknown geometry of the methanol distribution this number should not be taken too seriously, although we note that methanol column densities of similar magnitude have been observed toward a number of other star forming regions (Menten et al. 1986).

4.1.4. DR 21

Menten et al. (1986) detected methanol emission at a velocity of -2.6 km s^{-1} in the 25 GHz $J_2 \rightarrow J_1 E$ lines toward a position about 75″, corresponding to ≈ 1 pc, west of the DR 21 radio continuum/infrared source complex (Wynn-Williams et al. 1974). Subsequently, maser emission in the $4_{-1} \rightarrow 3_0 E$ and $7_0 \rightarrow 6_1 A^+$ transitions was detected by Haschick et al. (1990) toward the

Table 2. Sources toward which no emission was detected

Source	α_{1950}	δ_{1950}	v^{a}_{LSR} (km s^{-1})	ΔS^{b} (Jy)
IRAS 00117+6412	$00^{h}11^{m}44^{s}.9$	64°11′50″	−38	11
IRAS 00211+6549	00 21 09.6	65 49 26	−38	11
NGC 281	00 49 29.2	56 17 36	−32	7
S Per	02 19 15.1	58 21 34	−37	10
W 3(OH)	02 23 17.0	61 38 54	−47	15
W 3−2	02 21 53.1	61 52 22	−40	10
W 3	02 21 55.0	61 54 00	−41	9
IRAS 02395+6244	02 39 31.0	62 44 16	−70	12
S 201	02 59 22.4	60 16 12	−33	9
CRL 490	03 23 38.7	58 36 38	−15	11
IRAS 03245+3002	03 24 33.9	30 02 36	10	9
HH 7−11 B	03 25 56.6	31 05 19	7	6
NGC 1333	03 26 00.9	31 05 35	7	8
HH 6	03 26 05.6	31 08 13	8	10
B 1	03 30 16.5	30 57 26	7	10
IC 348	03 40 50.7	31 52 26	9	17
S 209	04 06 24.7	50 52 08	−54	9
S 211	04 32 24.0	51 06 00	−41	12
IRAS 04361+2547	04 36 09.8	25 47 41	9	8
BFS 44	04 48 00.0	45 30 31	−27	9
G 173.58	05 36 06.4	35 39 21	−16	9
IRAS 05412−0104	05 41 18.6	−01 04 17	3	14
NGC 2071	05 44 30.0	00 20 40	8	10
S 241	06 00 40.9	30 14 54	−7	12
Mon R2	06 05 17.0	−06 22 40	−2	9
Mon R2−3	06 05 21.7	−06 22 35	12	12
S 270	06 08 01.0	12 33 25	25	10
GGD 12−15	06 08 26.0	−06 10 50	−16	8
S 256	06 09 31.4	17 56 25	5	8
S 255 B	06 11 29.0	17 46 10	10	12
S 269	06 11 46.3	13 50 31	18	7
S 266	06 14 32.8	17 56 25	35	15
G 195.8	06 15 50.0	15 06 09	21	20
S 283	06 35 54.6	00 47 20	57	14
S 284	06 42 36.0	00 25 00	43	13
G 212.25	06 43 41.7	00 09 34	38	11
S 286	06 52 06.1	−04 38 22	49	14
CRL 1074	07 05 28.5	−10 39 18	43	14
VY CMa	07 20 55.0	−25 40 12	19	20
S 305	07 27 43.2	−18 21 41	36	16
BBW 33	07 27 54.9	−20 37 45	72	17
CRL 1141	07 30 47.6	30 37 13	4	7
OH 0739	07 39 58.9	−14 35 38	21	14
X Hya	09 33 06.9	−14 28 02	28	15
R Leo	09 44 52.6	11 39 44	−1	11
R Crt	10 58 06.0	−18 03 21	4	16
S Crt	11 50 12.0	−07 19 00	38	14
U CVn	12 44 56.7	38 38 53	−22	10
RT Vir	13 00 05.7	05 27 22	22	11
AY Vir	13 49 16.0	03 25 48	−41	10
RU Hya	14 08 42.0	−28 38 24	−2	24
RX Boo	14 21 56.6	25 55 50	6	10
RS Vir	14 24 46.0	04 54 09	−14	12
S Crb	15 19 21.0	31 32 48	1	12
U Her	16 23 34.9	19 00 18	−15	13
IRAS 16293−2422	16 29 21.0	−24 22 16	6	18

Table 2 (continued)

Source	α_{1950}	δ_{1950}	v^{a}_{LSR} (km s^{-1})	ΔS^{b} (Jy)
NGC 6334 A	17 16 57.8	−35 51 45	−11	52
Sgr A−G	17 42 27.0	−29 04 36	45	46
G 6.55	17 57 47.4	−23 20 29	12	20
G 5.48	17 55 58.6	−24 20 43	22	22
G 8.14	18 00 00.2	−21 48 15	18	17
G 5.97	18 00 36.4	−24 22 54	11	18
G 10.15	18 06 22.5	−20 20 05	10	16
G 12.21	18 09 43.7	−18 25 09	10	15
M 17 L	18 17 27.0	−16 14 54	20	15
G 19.07	18 23 58.5	−12 28 17	63	13
G 20.08	18 25 23.2	−11 30 45	46	16
G 23.71	18 31 10.3	−08 09 36	110	12
G 23.96	18 31 42.6	−07 57 11	81	13
G 25.72	18 35 21.6	−06 26 27	98	14
G 27.28	18 37 55.7	−05 00 35	35	15
G 30.54	18 44 23.0	−02 10 43	40	16
G 31.41	18 44 59.4	−01 16 04	101	13
W 43−M4	18 45 32.8	−02 00 17	94	14
G 37.55	18 57 46.8	03 58 59	85	15
G 35.20	18 59 14.0	−01 09 03	45	16
W 48	18 59 15.0	−01 08 50	43	21
G 40.62	19 03 34.9	06 41 51	35	23
W 49 S	19 07 58.2	09 00 03	10	10
OH 43.8	19 09 31.2	09 30 51	41	9
G 44.26	19 09 34.1	10 01 57	57	14
G 43.18	19 09 44.8	08 47 03	56	10
G 45.07	19 11 00.4	10 45 43	60	9
G 45.12	19 11 06.2	10 48 26	60	11
G 45.48	19 11 47.5	11 07 14	52	11
G 45.49	19 11 50.0	11 07 47	63	17
G 43.89	19 12 02.8	09 17 19	55	9
G 45.47	19 12 04.3	11 04 11	60	13
G 50.31	19 19 11.4	15 38 37	50	8
G 50.23	19 20 18.2	15 24 21	50	12
W 51 N	19 21 22.4	14 25 13	33	23
G 54.10	19 29 29.3	18 36 26	44	13
S 87	19 44 14.0	24 27 58	26	15
S 88	19 44 40.0	25 05 00	30	15
G 61.48	19 44 43.5	25 05 22	25	12
K 3−50	19 59 50.1	33 24 17	−20	10
ON 3	19 59 58.4	33 25 47	−19	17
G 75.83	20 19 47.3	37 21 26	−6	6
S 106	20 25 27.0	37 12 45	1	9
G 97.53	21 30 37.0	55 40 36	−72	12
CRL 2789	21 38 10.6	50 00 43	−50	13
TW Peg	22 01 41.0	28 06 30	−8	13
S 146	22 47 31.0	59 39 30	−60	10
Cep A	22 54 19.2	61 45 44	−5	7
S 152	22 55 38.0	58 33 02	−52	11
IRAS 23004+5642	23 00 23.6	56 41 14	−50	11
S 156 A	23 03 05.0	59 58 10	−51	17
S 157	23 13 53.1	59 45 18	−46	14

[a] The velocity coverage of the filter bank spectrometer is ±43 km s^{-1}, centred on the LSR velocities given here

[b] 3σ upper limits on flux density in observed velocity range. The velocity resolution was 0.34 km s^{-1}

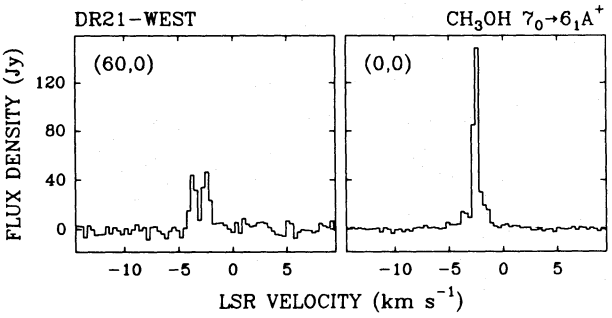

Fig. 2. Spectra of the $7_0 \rightarrow 6_1 A^+$ line of CH_3OH observed in the vicinity of the DR 21 region. The spectrum on the right hand side, labelled (0, 0) was taken toward the position of the maser DR 21-West found in the 25 GHz $J_2 \rightarrow J_1 E$ methanol transitions of CH_3OH, which is located $\approx 75''$ west of the DR 21 H II region. The spectrum on the left hand side was taken toward a position 60″ east of the 25 GHz maser position. The velocity resolution is 0.34 km s^{-1} for both spectra

same position. Our spectrum (Fig. 2) shows an additional feature at a velocity of -3.7 km s^{-1}, not seen in the $7_0 \rightarrow 6_1 A^+$ spectrum of Haschick et al. From offset observations we find that the -3.7 km s^{-1} component is located at an offset of (87″, 6″) relative to the position of the -2.6 km s^{-1} feature. The errors in the relative position determination are 10″ in both coordinates. This large offset, much bigger than the 44″ beam of Haschick et al.'s observations, explains the latter authors' non-detection of the -3.7 km s^{-1} feature.

4.1.5. NGC 7538

Our detection of a strong maser with a peak intensity of ≈ 43 Jy (Table 1, Fig. 1) toward the infrared source IRS1 in the NGC 7538 region on first look does not appear to be in agreement with the upper (3σ) limit of 15 Jy obtained by Haschick et al. toward the same position. However, from our five-point map measured at offsets of $(\Delta\alpha, \Delta\delta) = (0, 0)$, $(\pm 1', 0)$, and $(0, \pm 1)$ relative to the position listed in Table 1, we estimate that the maser position is offset by $(14'' \pm 4'', -37'' \pm 3'')$ from the IRS 1 position. The errors given represent the formal uncertainties that result from fitting a Gaussian source model to the measured intensities. Since the observations of Haschick et al. were made with a beam size of 46″ at 44 GHz, their non-detection is perfectly understandable, especially if one considers the combined pointing uncertainty of their and our observations, which is of order 25″. In fact, Haschick et al. report emission toward NGC 7538S, offset by $(-4'', -79'')$ from our (and their) NGC 7538 position between velocities of -58 and -52 km s^{-1}. Their signal-to-noise ratio is rather poor and it is difficult to decide whether the observed emission consists of one broad features or several narrow components, but clearly emission is present at -57 km s^{-1}, the velocity of the maser feature observed by us.

Our detection represents the first measurement of a Class A methanol maser in the NGC 7538 region. The ultra-compact H II region associated with the infrared source IRS 1 (Campbell, 1984), located at the position given in Table 1, is a well studied Class B methanol maser source showing strong maser emission in the 12 GHz $2_0 \rightarrow 3_{-1} E$ transition. VLBI measurements by Menten et al. (1988b) have shown that the 12 GHz masers appear projected on the H II region and emerge from the same region as the OH masers. Like in the prototype Class B source W 3(OH), the 25 GHz $J_2 \rightarrow J_1 E$ transitions appear in absorption against the continuum source (Menten et al. 1986). It is interesting to note that the latter authors also measured a five-point map with a spacing of $\pm 40''$ (i.e. a full beamwidth) around the continuum position, but do not report the detection of narrow *emission* toward any of these positions. It thus seems that the $7_0 \rightarrow 6_1 A^+$ maser does not have a 25 GHz counterpart.

4.2. *General properties of the observed methanol masers*

It is clear from our observations that the detected methanol masers are found in regions of on-going star formation, since H_2O masers, ultracompact H II regions, and molecular outflows are observed near to the methanol maser positions. Our coarse spatial resolution prohibits a detailed comparison of the methanol positions with positions of these other phenomena, but we mention that in some case (DR 21, NGC 7538) we have clear evidence that the methanol masers are not coincident with the ultracompact H II regions present in their neighborhoods.

Interestingly, H_2O masers have also been observed at considerable offsets from compact H II regions. In particular, recent observations conducted with the Nobeyama Millimeter-wave Interferometer (Kameya et al. 1989) found 4 not previously known water masers at offsets of several arc minutes from the known compact IR and continuum sources in the NGC 7538 region. We note however, that the relationship between Class A methanol masers and water masers is unclear at present. Certainly methanol masers do not show the multitude of velocity features present in H_2O spectra over wide velocity intervals. The velocities of the few features found in Class A methanol masers are the same as those of the thermal molecular lines in the same regions, to within a few km s^{-1}.

It is well known that in a number of regions the methanol masers are spread over large areas. For example, in the W 51 region Menten et al. (1986) found emission in the 25 GHz lines from five different positions distributed over a $2' \times 2'$ area, corresponding to 5×5 pc, that also have counterparts in the $7_0 \rightarrow 6_1 A^+$ line (Haschick et al. 1990). In the DR 21/W 75 region, the Class A masers have been found near DR 21, DR 21(OH) (= W 75S), W 75 S(3), and, somewhat further away, W 75N, and are thus spread over similar distances. Many more Class A masers may remain undetected, since unbiased surveys of molecular cloud regions away from known IR and compact continuum sources and other molecular masers have never been made.

4.3. *Future observations*

It would certainly be interesting to search for emission from other known Class A methanol maser lines towards the positions where we detected masers in the $7_0 \rightarrow 6_1 A^+$ transition. Such observations in principle can yield important information on the excitation of Class A methanol masers (see Haschick et al. 1990), since any conceivable pumping scheme will have to explain the simultaneous inversion of several transitions in one and the same region. In fact, Haschick et al. (1990) found that many of their detected 44 GHz masers have counterparts in the 36 GHz $4_{-1} \rightarrow 3_0 E$ and the 25 GHz $J_2 \rightarrow J_1 E$ transitions (see also Sect. 4.1.4 above). To our knowledge, most of the regions where we detect new masers in the 44 GHz transition have never been

observed in any methanol line before and future surveys of several transitions would be of great interest.

5. Conclusions

We have searched for emission in the $7_0 \rightarrow 6_1 A^+$ transition of CH_3OH toward a sample of 124 known water masers associated with star forming regions and evolved stars. Emission was detected toward 16 sources, all of which are located in the general vicinity of compact H II regions. In most cases maser action is observed, indicated by narrow, intense spectral features.

Sources showing maser emission in the $7_0 \rightarrow 6_1 A^+$ line are Class A methanol masers, and thus frequently found offset from other molecular masers, compact H II regions and infrared sources.

The methanol maser velocities are similar to the systemic velocities of the regions in question. No high-velocity features are observed.

Our relatively large beamwidth of 2′ enabled us to detect several new maser components in regions that where previously known to be methanol maser sources (DR 21, NGC 7538). Higher spatial resolution studies are needed to allow meaningful comparisons with other phenomena that are present near the methanol masers.

Acknowledgements. We would like to thank the anonymous referee for a careful reading of the manuscript.

References

Batrla W., Matthews H.E., Menten K.M., Walmsley C.M., 1987, Nat 326, 49
Batrla W., Menten K.M., 1988, ApJ 329, L117
Campbell B., 1984, ApJ 282, L27
Cesaroni R., Palagi F., Felli M., Catarzi M., Comoretto G., Di Franco S., Giovanardi C., Palla, F., 1988, A&AS 76, 445
Felli M., Johnston K.J., Churchwell E., 1980, ApJ 242, L157
Genzel R., Downes D., 1977, A&AS 30, 145
Güsten R., Fiebig D., 1988, A&A 204, 253
Harvey P.M., Forveille T., 1988, A&A 197, L19
Haschick A.D., Baan W.A., 1989, ApJ 339, 949
Haschick A.D., Baan W.A., Menten K.M., 1989, ApJ 346, 330
Haschick A.D., Menten, K.M., Baan W.A., 1990, ApJ 354, 556
Kameya O., Morita K.-I., Kawabe R., Ishiguro M., 1990, ApJ 355, 562
Menten K.M., 1987, Doctoral Thesis, University of Bonn
Menten K.M., Walmsley, C.M., Henkel C., Wilson T.L., 1986, A&A 157, 318
Menten K.M., Johnston, K.J., Wadiak E.J., Walmsley C.M., Wilson T.L., 1988a, ApJ 331, L41
Menten K.M., Reid M.J., Moran J.M., Wilson T.L., Johnston K.J., Batrla W., 1988b, ApJ 333, L83
Menten K.M., Walmsley C.M., Henkel C., Wilson T.L., 1988c, A&A 198, 267
Morimoto M., Ohishi M., Kanzawa T., 1985, ApJ 288, L11
Norris R.P., Caswell J.L., Gardner F.F., Wellington K.J., 1987, ApJ 321, L159
Oliva E., Moorwood A.F.M., 1986, A&A 164, 104
Plambeck R.L., Wright M.C.H., 1988, ApJ 330, L61
Wilson T.L., Walmsley C.M., Snyder L.E., Jewell P.R., 1984, A&A 134, L7
Wilson T.L., Walmsley C.M., Menten K.M., Hermsen W., 1985, A&A 147, L19
Wynn-Williams C.G., Becklin E.E., Neugebauer G., 1974, ApJ 187, 473
Wood D.O.S., Churchwell E., 1989, ApJS 69, 831